Electrochemical Corrosion of SnO_2:F Transparent Conducting Layers in Thin Film Photovoltaic Modules

C.R. Osterwald, T.J. McMahon, and and J.A. del Cueto

National Renewable Energy Laboratory

1617 Cole Blvd.

Golden, CO 80401-3393 USA

Abstract

We report on a degradation mechanism in thin-film photovoltaic (PV) modules activated by damp heat and voltages similar in magnitude to those generated by PV modules in power generation systems. This mechanism, which appears to be an electrochemical process involving the soda-lime glass superstrate with its conductive SnO_2:F layer, can be greatly accelerated by subjecting modules to elevated temperatures and humidity, both of which increase the leakage currents between the frame and the active PV layers. Water vapor can affect the module damage in two ways: 1) by enhancing leakage currents, and 2) by entering through the module edges, it appears to promote the chemical reaction responsible for the SnO_2 corrosion. Damage has been found to occur in both a-Si and CdTe modules.

Keywords: Thin-film modules; Electrochemical corrosion; Tin oxide; Leakage currents

1. Introduction

A common method of fabricating thin-film PV modules begins with a superstrate of soda-lime glass that has been coated on one surface with a thin layer of tin oxide doped with fluorine (SnO_2:F). The transparent conductive oxide (TCO) forms the top contact for the solar cell layers that are, in turn, deposited on the tin oxide (Fig. 1). Laser groove patterning is used to define individual solar cells in the shape of narrow strips that extend across one dimension of the module; the cells are connected in series to increase the output voltage. Because tin oxide extends across the entire front surface, additional processing is needed to remove it in the gap between the edges of the cells and the edges of the glass; this process is known as an "edge delete." A polymer encapsulant, ethylene vinyl acetate (EVA), provides both electrical isolation between the solar cells and the outside, and bonds the glass backsheet to the rest of the module. Lastly, an extruded aluminum frame around all four edges provides structural mounting points, protection for the glass edges, and the electrical grounding point. A bead of butyl rubber forms a buffer between the frame and the glass, and provides additional adhesion for the frame. Not all thin-film modules have metallic frames, however; other designs use mounting points bonded to the backsheet instead. As we shall show, this is an important difference.

Photovoltaic manufacturers usually do not produce the SnO_2:F layers used in thin film modules themselves; rather, the coatings are applied by the glass manufacturers, who then sell the coated superstrates as a complete product [1]. As supplied, the tin oxide coatings are very hard (harder than the glass itself) and difficult to remove. For this reason, the edge delete has been performed using a number of different processes, including laser scribing and abrasive removal.

Thin-film superstrate modules in this configuration have a major construction difference when compared to crystalline Si modules, which require no SnO_2 on the front glass and use an additional layer of EVA between the glass and the front surface of the solar cells. The extra EVA layer therefore provides electrical isolation that is not available to thin-film modules, which is an important difference because leakage currents through the glass superstrate or the module edges can easily reach the active semiconductor layers.

Leakage currents and electrochemical corrosion in PV modules have been studied in the past by the Jet Propulsion Laboratory (JPL) [2, 3]. The stress test used in [3] to accelerate the corrosion was to place the test module in high-humidity (85% relative humidity [RH]) at high temperatures (+85°C), while 500 V was applied between the metallic frames and the shorted module output leads, in both polarities. For modules connected in series to increase operating voltages in power generation systems, potentials of several hundred volts at the end of a series string and the system ground are common. With the exception of the voltage bias, this test is similar to the so-called 1000-h damp-heat test that is part of the standard PV module qualification test sequence [4]. Although the damp-heat test is an extreme stress when compared to actual operating conditions, it was included in the standard qualification sequence because it was found to uncover known failure mechanisms. Modules that are not constructed properly will often develop delamination or discoloration of the polymers from moisture ingress during damp heat.

Electrochemical corrosion of amorphous silicon (a-Si) PV modules has been reported previously. Firstly, in reference [5], it was observed in modules deployed in two small grid-connected PV systems that operated at about 200 Vdc. The authors stated that “newer modules with better edge

seals, and/or modules with nonconducting frames have not yet shown this defect." The effect was called "bar graph" corrosion because of the tendency to progress from the module edges inward along individual a-Si solar cells. Secondly, JPL produced similar corrosion under laboratory conditions [6], and reported that the effect was caused by a reaction involving H_2O that converted SnO_2 to nonconductive SnO, which delaminated from glass surfaces. Note that these tests involved placing glass plates coated with SnO_2 in HCl, rather than using actual modules. The authors concluded that "sample anodes tended to delaminate at the glass/TCO interface due to chemical attack of the glass itself." Thirdly, corrosion in thin-film modules has also been reported more recently [7], but only briefly and in a different context.

2. Accelerated Testing

In light of this history, we have employed the JPL biased damp-heat test to determine if newer thin-film modules are susceptible to damage from high voltage. The test voltage was raised to 600 V, however, because this is the maximum system voltage for which commercial modules are currently rated. Two identical modules, each a-Si glass superstrate modules 660 mm wide by 1220 mm long, were placed in an environmental chamber capable of controlling temperature and humidity, and +600 V relative to the frame was applied to the shorted output leads of one module, while −600 V was applied to the other module. The leakage currents flowing in these circuits were monitored during the testing. Typically, the leakage currents would reach maximum values when the chamber completed ramping to the desired environmental conditions, and then slowly decrease with time. Table 1 summarizes the accelerated testing for the modules subjected to the negative-polarity bias voltage.

For the a-Si modules used in this study, several hundred hours at 85°C, 85% RH, and −600 V bias would typically result in visible damage, such as that recorded in Fig. 2. Modules subjected to the positive bias show very little damage. The corrosion normally starts at the ends of the individual solar cells and progresses inward, and is preferential to some cells as other cells have no damage at all, i.e., "bar graphing." One or two of the visible hair-like tendrils begin forming at the cell edges or the scribe lines, and as the corrosion progresses, the damage becomes dense and threaded. Examination of the damaged areas under a low-power optical microscope shows that the tendrils seem to be cracks through all of the thin-film layers, including the TCO, the active semiconductors, and the back metallization. This was verified by observing that visible light can be transmitted through the cracks and both glass sheets, as seen in Fig. 3 (the back metallization is normally opaque). Additional examination of areas damaged by the high-voltage stress shows the normally durable SnO_2:F now has very little adhesion to the glass. This change is drastic enough that the damage has also been called a delamination.

The exact chemical reaction responsible for the damage is not yet known, but the strong dependence on the polarity of the bias voltage suggests that Na^+ ions may be migrating from the glass to the SnO_2 layer and possibly reacting with the fluorine. This reaction may also need H_2O in some form because of the rapid acceleration that occurs under high humidity conditions. In an attempt to determine if Na^+ ion migration is a key component in this mechanism, a number of test modules were made with borosilicate glass rather than soda-lime. Under biased damp heat conditions, these modules did not suffer any visible corrosion effects [8]. This is a strong indication that sodium is needed, in contrast to the reactions reported by JPL [6].

Although the damage that occurred under positive bias polarity with respect to the frame was small, it was not zero. This module design used a laser scribe through the tin oxide 2 mm wide and 8 mm from the edges to isolate the individual solar cells from the outside. All of the damage occurred outside of this edge delete, whereas in the negative case, all damage was inside the scribe. We speculate that the positive-bias case uses reactants already available at the surface, rather than needing mobile ions from the glass topsheet. This would imply that contamination of the topsheet surface prior to encapsulation should be minimized.

3. Temperature Dependence of Damage

Because the damage is so apparent with a visual inspection, area is a convenient way to measure the progress of the damage. In succession, we then subjected three identical modules to −600 V and 85% RH, at a temperature of 85°, 72°, or 60°C; module leakage currents were measured during exposure. At periodic intervals, the modules were removed from the environmental chamber and the damage area measured. Fig. 4 shows the damage as a percentage of the PV active module area versus time. It should be noted that the chamber required about 3 h to ramp the temperature and humidity up to the test values; the ramp times were not considered in Fig. 4. In addition to the strong temperature dependence, Fig. 4 shows a time threshold for the damage to begin. Below the threshold, very little visible damage occurs, and above the threshold, the damage is nearly linear. The thresholds complicate the calculation of the activation energy; as a solution, we plotted the slopes of least-squares fits to the linear portions of Fig. 4 in an Arrhenius plot, which is shown in Fig. 5. The activation energy obtained was 0.78 eV, although this result is probably only applicable for this particular a-Si module design.

Knowing the leakage currents during the exposure tests allowed the total charge transferred through the modules to be calculated, and Fig. 6 shows the damage area versus the time-integrated leakage currents (Table 1 also lists the total charge transferred to the modules by leakage currents). Figure 6 again shows the damage threshold, and the three curves are much closer together than those in Fig. 4. Note that after the threshold, the three curves are roughly linear with similar slopes, even though the actual leakage currents are slowly decreasing in magnitude. In Fig. 6, for a fixed amount of charge transfer, damage at a lower temperature is reduced, so both the leakage current and the damage mechanism are thermally activated.

4. Materials Dependency and Leakage Currents

To determine if the materials in active photovoltaic layers have any affect on the damage, we performed the accelerated corrosion test on two cadmium telluride (CdTe) modules, one at each polarity. These modules were also double-glass superstrate structures, and differed only in the CdTe solar cells and the lack of a frame around the outside edges (these modules had disks bonded to the backsheet for mounting points that are also used for grounding). Over 500 h at 85°C and 85% RH resulted in no visible damage.

Following this test, we were unable to determine if the negative result was due to the PV materials or the lack of an outside frame. As an attempt to isolate these two possibilities, we used two approaches. First, an aluminum frame was removed from an a-Si module and installed on another CdTe module along with the butyl rubber edge protection. Second, to investigate the frameless case for a-Si, we simulated the backsheet mounting scheme by bonding a metallic ground point with silicone to the rear surface of the now-frameless a-Si module. Both modules

were tested at the same time. The test was performed at 72°C to slow the rate of damage and observe the changes.

As seen in Table 1, the leakage currents for the a-Si module were reduced by almost two orders of magnitude, and no visible damage was evident after 1200 h of exposure. For the CdTe module, however, damage to the SnO_2 similar to that previously observed in a-Si modules was visible. Note that the CdTe module used a 10-mm-wide mechanical edge delete along the entire length of the glass edges, as opposed to the 2-mm-wide laser scribe for the a-Si, which may be the reason for the reduced amount of damage for the CdTe case. These results indicate that the metallic frame around the edges plays a key role in enhancing the leakage currents that are necessary for the SnO_2 corrosion, and the duplication of the previous results with the frames switched shows that the process occurs in both CdTe and a-Si. Therefore, we believe that the damage only involves the SnO_2 and does not depend on the photovoltaic absorber materials.

These results show that for both CdTe and a-Si, damage only occurred in framed modules, which agrees with the observation reported in reference [5]. Considering the possible current paths in comparison to a framed module as shown in Fig. 1, a frameless module will likely have only a path through both the bulk EVA and the glass backsheet. Reference [3] contains temperature and humidity dependencies of surface and bulk electrical conductivities for both EVA and soda-lime glass. Using these data, we estimated the contribution of several of the currents identified in Fig. 1 to the total leakage current (I_4 and I_5 were not included because these currents associated with the backsheet are much smaller than the first three). These calculations are presented in Table 2.

The success in duplicating the damage results in CdTe led to another question—can the corrosion be stopped even if a module has a metallic frame? While considering this question, we wondered what the role of the butyl rubber edge protection might be. To investigate this issue, the frame on an a-Si module was removed, the butyl rubber was replaced with silicone rubber between the frame and the glass, and the frame was reinstalled. The results of this test are presented in Table 1, which shows that the leakage currents were reduced by an order of magnitude with very little corrosion, even after 1200 h of exposure. Thus, we concluded that acceptable results can be obtained even with a frame if the leakage currents associated with the frame are controlled.

Reference [2] used the total charge transferred by leakage currents divided by the module edge perimeter length as a gauge. It was found that 50% a-Si module output power losses can be expected when 10 to 100 C/m of charge have been transferred at 500 V, 85% RH, and 85°C (note that this study did not vary temperature). Comparing these charge-transfer amounts to the first three modules listed in Fig. 6, which have a perimeter length of 3.75 m, we measured 40% to 50% power losses when only 1 C/m has passed. Considering that the total leakage current will include contributions from both the edge and the superstrate, it is difficult to justify normalizing the total charge transferred by the perimeter length alone. Also, from our experience, the figure of merit in [2] should vary with temperature, as well as from module to module. Thus, we cannot recommend its use.

Similar a-Si superstrate modules have been biased to ±600 V while deployed outdoors to simulate the environment a module might encounter as part of a large PV array [9]. During a

three-year exposure period, an a-Si module received a total of about 7 C of charge while biased in the negative polarity, but suffered just 0.4% damage over the active area. This amount of charge is larger than that received by any of the chamber-stressed modules, yet the amount of damage is much less. The leakage currents reported in reference [9] were about 0.05 to 5 μA, which are an order of magnitude smaller than the highest values measured in the chamber testing. The outdoor leakage currents are not causing damage at the same rate, probably because, overall, the temperatures are much lower. This result also implies that the temperature dependence of the leakage currents is not equal to the temperature dependence of the damage rate. Finally, the outdoor result demonstrates that the process is not an artificial one seen only under extreme conditions.

5. Water Vapor

We then attempted to separate the influence of the high water vapor environment on the effect. For a first experiment, an unmodified a-Si module was placed in the environmental chamber and biased to −600 V at 85°C, but without water vapor. This module, #1148 in Table 1, had leakage currents nearly an order of magnitude smaller than those of #2020, and displayed a damage area of only 0.2% after an exposure time that was twice as long. It can therefore be seen that the presence of water vapor greatly accelerates the damage rate, but its absence or near-absence does not completely eliminate the effect.

Table 2 indicates that currents I_1 and I_2 are the strongest leakage paths into the module. After observing the strong effect that edge currents have when a metallic frame is present, we wanted to determine if the corrosion can occur via leakage currents through the glass superstrate when a

frame is not present. To test this possibility, we used the same a-Si module that had its frame removed and had been exposed at the same time as the CdTe (#8221). Three small (15 × 30 mm) aluminum contacts were bonded to the front surface and connected to the positive output of the high-voltage supply. Several hundred hours of 85°C, 85% RH resulted in a small amount of corrosion directly under two of the three contacts.

Next, we removed the frame from a fresh a-Si module and replaced it with two aluminum channels bonded to the front glass. These channels extended inward from one edge (10 × 310 mm) and from one corner (10 × 450 mm) to the center of the module. It was hoped that this configuration would show a progression of damage as water vapor migrated inward from the edges. In an attempt to minimize any water vapor already inside, the module was first tested at 85°C without humidity. As listed in Table 1, module #7016 was exposed in this condition for over 600 h. In contrast to the framed module without humidity (#1148), the leakage currents were quite small, only 20 nA, and no damage was observed.

Finally, #7016 was placed in 85°C, 85% RH, at −600 V. The leakage currents were almost three orders of magnitude higher, and a large amount of corrosion occurred after just 170 h. Unlike the earlier attempt with the three small contacts, there was no apparent correlation of the corrosion pattern to the aluminum channels on the front; the pattern instead looked very much like those seen previously in framed modules. Because the current increased immediately with the addition of water vapor, it is likely that water on the front surface is responsible for the increase (i.e., current I_1 has been enhanced).

Fig. 7 summarizes the three different bias configurations used for the accelerated testing and the resulting electric field directions (these configurations were separate, not simultaneous). This illustration shows that for the backsheet ground configuration, V_{bias3}, positive ions in the glass must penetrate the EVA, the solar cell back metallization, and the active PV layers before they can reach the tin oxide. In contrast, in the other two configurations, V_{bias1} and V_{bias2}, electric fields are present that give paths directly to the TCO from the glass superstrate.

After considering all of these results, we suspect that water vapor affects the corrosion of SnO_2 in two ways. First, water vapor ingress through the module edges may be required for the electrochemical reaction, and second, water vapor increases the conductivity of the front glass surface, thereby increasing the leakage currents, I_1, through the front and directly into the tin oxide. Evidence for the first effect can be seen in Fig. 2, where completely undamaged cells are adjacent to cells that have extensive corrosion. This may be caused by water vapor ingress rates that vary along the edges; presumably the undamaged cells have excellent H_2O barriers. Also, the cell laser scribing may play a part in directing water vapor into the module. Finally, with front contacts that extended a significant portion of the distance from the edges to the center, damage rates were observed that exceeded those of normal framed modules.

6. Summary and Conclusions

Using high-voltage biasing of PV modules inside an environmental chamber, we have studied electrochemical corrosion of SnO_2:F transparent conductor layers that occurs in thin-film modules. The exact chemical reaction that produces this corrosion is still unknown. From our results, we have made the following conclusions:

1) The corrosion depends on the direction of the internal electric fields; modules biased positively from the metallic frame to the active PV layers show very little damage.
2) Modules that lack a frame and use mounting points bonded to the backsheet glass show no damage.
3) Corrosion causes cracking that extends through all of the thin-film PV layers.
4) Water vapor enhances the corrosion if it can enter the module through the edges, and by increasing the conductivity of the front glass surface.
5) Damage has been found to occur in both a-Si and CdTe thin-film modules.
6) Damage rates can be slowed if leakage currents that are caused by voltage potentials between the frame and the internal circuitry are reduced.
7) For the particular a-Si module design studied, the thermal activation energy of the damage area at 85% RH was 0.78 eV.
8) Both leakage currents and the damage for a given charge are thermally activated.

Acknowledgements

This work was supported by the U.S. Department of Energy under contract No. DE-AC36-99GO10337. We acknowledge the considerable efforts of coworkers at the National Renewable Energy Laboratory. Jim Pruett performed many hours of environmental chamber testing, and Steve Rummel and Alan Anderberg provided module current-voltage measurements.

References

1) G. Little, NREL Moisture Ingress and High Voltage Isolation Workshop, Golden, 2001.

2) G.R. Mon and R.G. Ross, Jr., Proc. 18th IEEE Photovoltaic Specialists Conference, Las Vegas, 1985, pp. 1142-1149.

3) G. Mon, L. Wen, R.G. Ross, Jr., and D. Adent, Proc. 18th IEEE Photovoltaic Specialists Conference, Las Vegas, 1985, pp. 1179-1185.

4) IEEE Recommended Practice for Qualification of Photovoltaic (PV) Modules, IEEE Std. 1262-1995, 24 p., ISBN 1-55937-586-8 (IEEE, New York, NY, 1996).

5) D.A. Fagnan, R.V. D'Aiello, and J. Mongon, Proc. 19th IEEE Photovoltaic Specialists Conference, New Orleans, 1987, pp. 1508-1509.

6) G. Mon, L. Wen, J. Meyer, and R. Ross, Jr., Proc. 20th IEEE Photovoltaic Specialists Conference, Las Vegas, 1988, pp. 108-113.

7) J.H. Wohlgemuth, M. Conway, and D.H. Meakin, Proc. 28th IEEE Photovoltaic Specialists Conference, Anchorage, 2000, pp. 1482-1486.

8) D.E. Carlson and F. Willing, private communication, 2001.

9) J.A. del Cueto and T.J. McMahon, Prog. Photovol.: Res. Appl. 10 (2002) 15-28.

Table 1.

A summary of the biased stress testing performed for this study. All modules were biased at −600 V with respect to the module frame or grounding point. The dashes in the maximum output power column indicate data that were not measured.

Sample	T/RH (°C, %)	Total Time (h)	I_L (μA)	Total Charge (C)	Damage Area (%)	Damage Rate (mm^2/h)	ΔP_{max} (%)	Comments
2020	85/85	230	17 → 3	4.6	14.8	450	-39.6	a-Si, framed
1051	72/85	400	3 → 2	2.9	10.9	240	-38.6	a-Si, framed
100	60/85	1340	3 → 1	5.6	8.3	67	-52.2	a-Si, framed
3006	85/85	510	10 → 7	18	0	0	—	CdTe, frameless
127	72/85	1240	8 → 5	32	4.3	24	—	CdTe, frame added
127	85/85	190	23 → 12	8.8	1	37	—	CdTe, frame added
8221	72/85	1240	0.2 → 0.05	0.3	0	0	—	a-Si, frame removed, back contact
8171	85/85	1190	2 → 0.9	4.4	1.4	97	-5.1	a-Si, silicone edge buffer
8221	85/85	360	0.2 → 0.12	0.16	0.08	0.6	—	a-Si, frame removed, front contacts
1148	85/0	470	7 → 0.7	3.1	0.2	2.7	—	a-Si, framed
7016	85/0	630	0.02	0.5	0	0	—	a-Si, frame removed, front contacts
7016	85/85	170	9 → 13	6.4	18	800	—	a-Si, frame removed, front contacts

Table 2.

Calculated individual currents for several of the paths identified in Fig. 1, with 600 V applied between the module frame and the TCO, using the physical dimensions of the a-Si modules in this study.

T/RH (°C, %) →	25 / 25	85 / 0	85 / 85 (dry EVA)	85 / 85 (wet EVA)
I_i (μA)				
I_1	0.026	3.5	12	12
I_2	0.048	5	5	30
I_3	0.0005	0.024	0.024	0.075
Total	0.075	8.7	17	33
Measured	0.01	0.7 – 7	19	3 – 19

Figure Captions:

Figure 1. A cross section of a PV module constructed with the SnO_2:F transparent conducting oxide (TCO) layer deposited on a glass superstrate. The active semiconducting layers are deposited over the tin oxide, and the entire package is encapsulated with ethylene vinyl acetate (EVA) between another sheet of glass. Not shown are the laser scribes that form the individual solar cells connected in series. Five possible current paths between the frame and the TCO are illustrated: 1) along the surface and through the bulk of the glass superstrate, 2) along the glass superstrate-EVA interface, 3) through the EVA bulk, 4) along the glass backsheet-EVA interface and through the EVA bulk, and 5) along the surface and through the bulk of the glass backsheet, and through the EVA bulk.

Figure 2. This photograph shows a portion of the front surface of a-Si module #2020 (see Table 1) after 200 h exposure at 85°C, 85% RH, and −600 V bias with respect to the module frame. The vertical stripes are the individual solar cells, which are 9.2 mm wide.

Figure 3. A micrograph of the damage on two adjacent solar cells with illumination on both the front and rear module surfaces. The three laser scribes that separate the solar cells are the horizontal lines across the center, each of which are about 100 μm apart. The bright flares are caused by transmission of the rear illumination through the cracks.

Figure 4. Percent of the active photovoltaic module area damaged as a function of time, for three different temperatures. The relative humidity inside the environmental chamber was 85%, and the shorted module output leads were biased to −600 V with respect to the module frame.

Figure 5. An Arrhenius plot of the slopes of the linear regions above the thresholds in Fig. 4.

Figure 6. Percent of the active photovoltaic module area damaged as a function of total charge transferred, for the same three modules used for Fig. 4. The total charge was calculated from a time integration of the module leakage current.

Figure 7. A representation of the electric field directions that result when each of three high-voltage bias configurations used in the accelerated testing are applied to the glass superstrate module illustrated in Fig. 1. Note that the front-contact configuration, V_{bias2}, is not part of a production module; it was an artificial configuration used for this study to determine the effects of leakage currents through the glass superstrate.

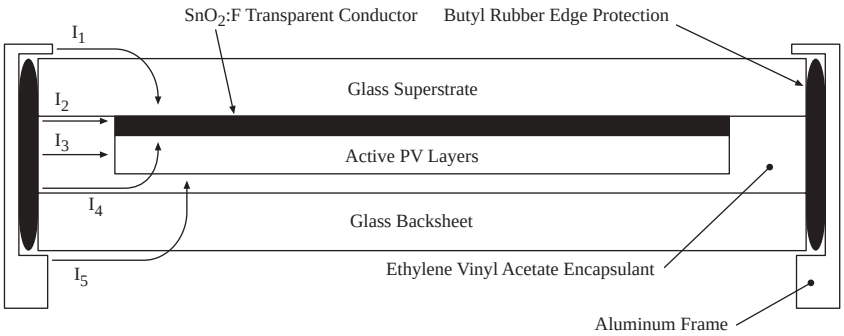

Figure 1

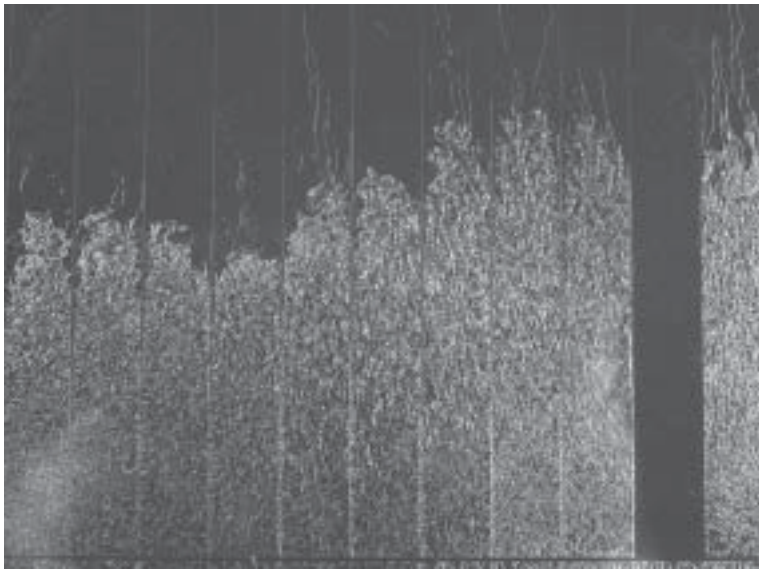

Figure 2

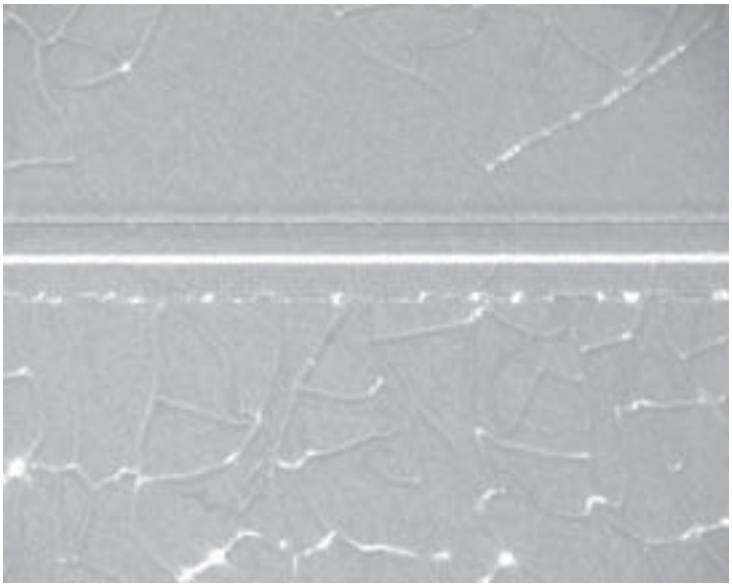

Figure 3

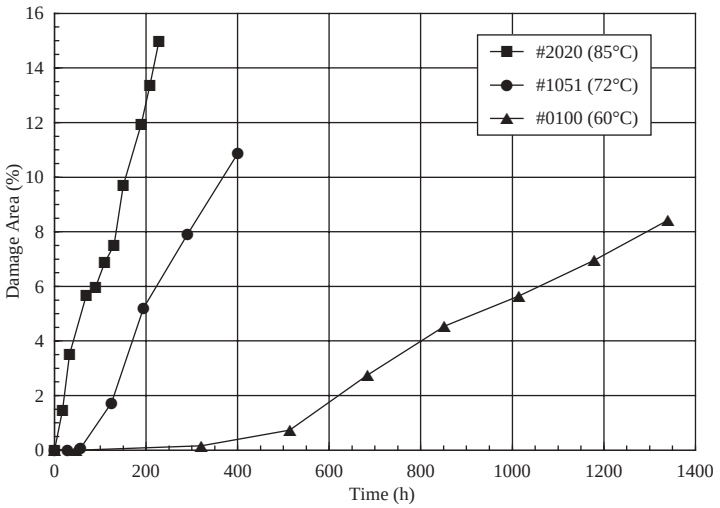

Figure 4

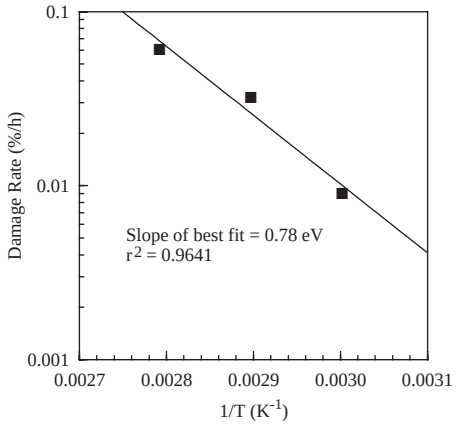

Figure 5

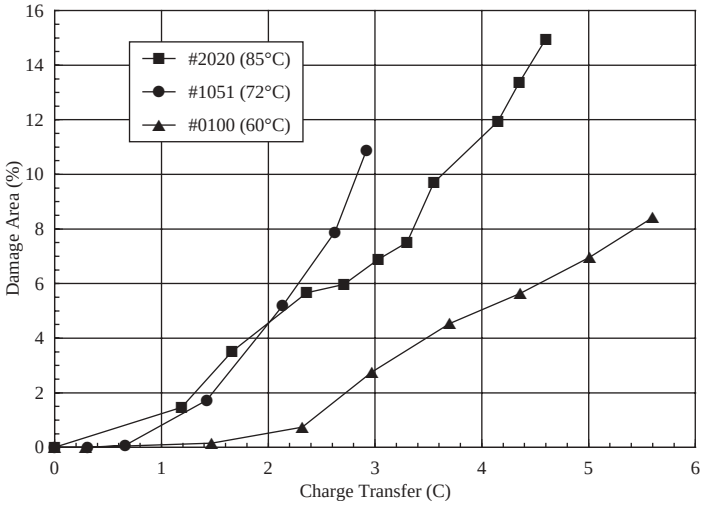

Figure 6

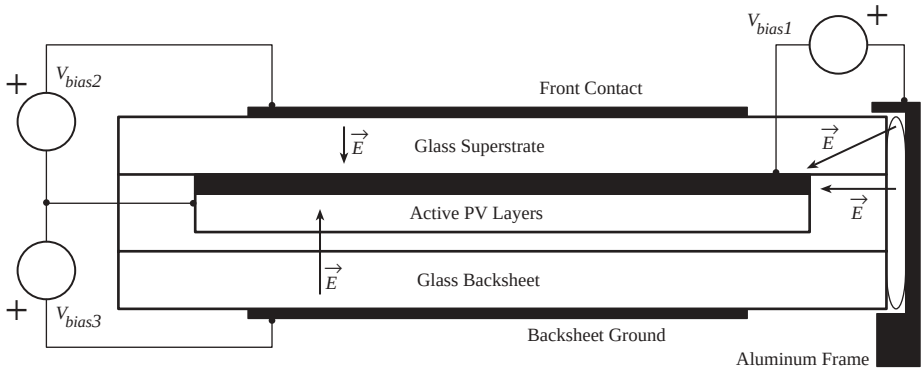
V_{bias1}
V_{bias2}
Front Contact
$\vec{E}$
Glass Superstrate
$\vec{E}$
Active PV Layers
$\vec{E}$
$\vec{E}$
Glass Backsheet
V_{bias3}
Backsheet Ground
Aluminum Frame

Figure 7